

Dynamics of the Milky Way Bar/Bulge

Ortwin Gerhard[✉]

Max-Planck-Institute for Ex. Physics, Giessenbachstr. 1, D-85748 Garching, Germany
email: gerhard@mpe.mpg.de

Abstract. Stellar surveys and dynamical models have recently led to important progress on understanding the dynamical structure of the Milky Way's bar and central box/peanut bulge. This talk briefly reviews the density structure of the bulge and bar from star count tomography, the cylindrical rotation of bulge stars, and the measurements of their stellar masses and pattern speed that have been obtained by fitting dynamical models to the combined star count and line-of-sight velocity data. Recent work deriving absolute proper motions throughout the bulge from the VIRAC survey and Gaia has led to a new 3D measurement of the barred bulge kinematics which is expected to greatly improve the dynamical models, and has already confirmed the relatively slow pattern speed ($\sim 40 \text{ km s}^{-1} \text{ kpc}^{-1}$) obtained from the previous dynamical and gas-dynamical modelling.

Keywords. Galaxy: structure; kinematics and dynamics; stellar content, dark matter; galaxies: evolution; formation

The Milky Way is a barred galaxy with a central box/peanut (B/P) bulge. Despite the fact that the stars in the Galactic bulge are mostly very old, pointing to an early formation, most of the bulge stars are part of the B/P bulge and must therefore have formed in the early Milky Way (MW) disk. The B/P bulge represents the inner parts of the Galactic bar, transiting to a flat ‘long bar’ at about 2–3 kpc from the center.

The best constraints on the three-dimensional structure of the bulge come from large samples of red clump (RC) stars for which individual distances can be estimated with $\sim 10\%$ accuracy. These stars show asymmetric distance distributions between positive and negative longitudes l as expected for an inclined bar, and a peanut-shaped density distribution with exponential density profiles, which for sightlines $|b| \gtrsim 5^\circ$ around $l = 0$ has characteristic double-peaked magnitude distributions (the ‘split RC’) (Stanek *et al.* 1994; McWilliam & Zoccali 2010; Nataf *et al.* 2010; Wegg & Gerhard 2013).

The planar long bar, while originally thought to be tilted with respect to the barred bulge (Hammersley *et al.* 2000; Benjamin *et al.* 2005), in more recent work combining data from several photometric surveys is consistent with having the same orientation as the bulge within a few degrees. Its half-length is found to be $R \simeq 4.6 \text{ kpc}$ for its 180 pc-scale-height component, but reaches further to $5.0 \pm 0.2 \text{ kpc}$ for the so-called superthin component that dominates at the largest radii (Wegg *et al.* 2015).

Radial velocity data in multiple fields from several spectroscopic surveys show that the B/P bulge rotates nearly cylindrically, for all stars with metallicities up to $[\text{Fe}/\text{H}] \sim -1$ on the ARGOS metallicity scale (Kunder *et al.* 2012; Ness *et al.* 2013, 2016; Zoccali *et al.* 2017). The cylindrical rotation is similar to B/P bulges in external galaxies (Molaeinezhad *et al.* 2016); it can be fitted well by N-body B/P bulge models, but cannot be fitted well with an additional slowly rotating, classical bulge with more than 25% of the bulge mass (Shen *et al.* 2010). The overall line-of-sight velocity dispersion profile decreases steeply with $|b|$. Metal-poor stars have flatter dispersion profiles both along $|l|$ and $|b|$.

With dynamical models fitted to both star count and radial velocity data, the main dynamical parameters of the Galactic bar and bulge have been constrained, such as its pattern speed, stellar mass, and dark matter fraction (Portail *et al.* 2015, 2017a, hereafter P17). These are made-to-measure (M2M) particle models that work by iteratively adapting an N-body system, based on ‘observing’ it just like the real Galaxy was observed, until it finally agrees with the data constraints. These models are well-suited for incorporating large numbers of data constraints and for modelling complicated dynamical systems such as barred galaxies. They can also be extended to model the metallicity-dependent dynamics in the joint gravitational potential (Portail *et al.* 2017b); this topic is summarized in Gerhard (2018).

From a set of models constructed for different values of the dynamical parameters, P17 obtained a best pattern speed for the bulge and bar of $\Omega_b = 39 \pm 3.5 \text{ km s}^{-1} \text{ kpc}^{-1}$, similar to (more uncertain) estimates from gas dynamics analysis (Sormani *et al.* 2015). This value of Ω_b is supported by recent work based on bulge proper motions (see talk by Sanders and poster by Clarke *et al.*) and radial velocities in the long bar (talk by Bovy) that all find similar values around $\Omega_b = 40 \text{ km s}^{-1} \text{ kpc}^{-1}$. Thus different measurements for this important parameter now appear to converge, putting the corotation radius of the MW bar around a galactocentric radius of $\sim 6 \text{ kpc}$.

The dynamical and stellar mass of the MW bulge and bar are constrained by the P17 models to within typically a few % and 5–10%, respectively. Their best model has a ‘photometric’ total Bulge plus Bar mass of $M_{bb} = 1.9 \times 10^{10} M_\odot$. Together with the inner disk, the combined stellar mass in the inner Galaxy (within $< 5.3 \text{ kpc}$) is found to be $\sim 65\%$ of the MW’s total stellar mass, i.e. the major part of the Milky Way’s stars are in the inner Galaxy. Because the stellar mass per RC star is based on independent constraints from star counts and microlensing (see, e.g., Gerhard 2018), the dynamical mass in the bulge region is found to be greater than the stellar mass, i.e., the best models require about $\sim 20\%$ of the mass in the bulge to be dark matter. Moreover, the upper limit on this number together with the rotation curve suggests that the dark matter distribution in the MW has a core or mild cusp; see P17 for more details.

With the recent availability of the VIRAC near-infrared proper motion catalogue (Smith *et al.* 2018), and by cross matching with the Gaia DR2 catalogue, it has become possible to obtain absolute proper motion (PM) maps across the entire bulge except in the most crowded and extincted regions in the Galactic plane (Clarke *et al.* 2019, Sanders *et al.* 2019, see also talk by Sanders). After careful foreground subtraction, Clarke *et al.* (2019) derived both both line-of-sight integrated, on-sky PM maps, and maps as a function of distance, using RC-magnitude as a proxy. Figure 1 compares the VIRAC PMs with previous data, showing the velocity dispersion σ_{μ_l} and σ_{μ_b} , their ratio, and the correlation $\sigma_{lb}/(\sigma_{\mu_l}\sigma_{\mu_b})$. The agreement with Rattenbury *et al.* (2007) in their fields is generally very good. Both dispersions increase towards the MW plane, and values at high positive l are larger than at high negative l , due to the superposition of the inclined bar with the disk. The correlation measurements also agree well, with a clear quadrupole signature visible in both data sets. The agreement of the data from Kozłowski *et al.* (2006) is less compelling but the main trends are comparable.

In addition to the second-order moments, the absolute VIRAC PM data also allow measuring the linear mean PM moments $\langle \mu_l^* \rangle$ and $\langle \mu_b \rangle$. The $\langle \mu_l^* \rangle$ is sensitive to the bar’s pattern speed and shows clearly distinct PMs for the two components of the split red clump. The pattern of $\langle \mu_b \rangle$ on the sky is a superposition from the pattern rotation of the bar and the streaming motions within it.

Clarke *et al.* (2019) also show that one of the best models of P17 for the barred bulge, with a pattern speed of $37.5 \text{ km s}^{-1} \text{ kpc}^{-1}$, is able to reproduce all the observed features in the VIRAC data impressively well, even though it was not fitted to these data.

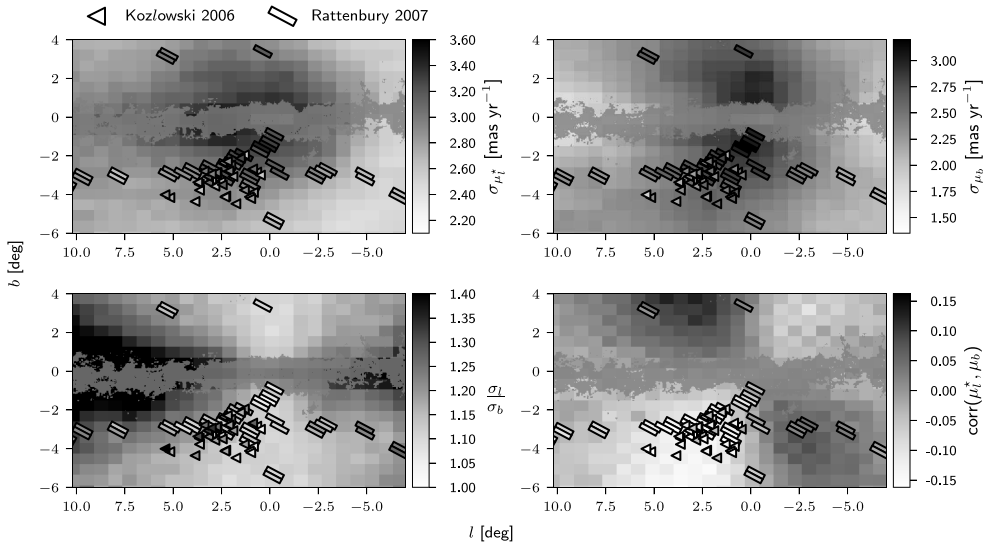


Figure 1. Comparison between VIRAC PMs and previous bulge PM studies (Kozłowski *et al.* 2006; Rattenbury *et al.* 2007). The panels show σ_{μ_l} and σ_{μ_b} , their ratio, and the PM correlation. The grey mask covers regions for which the extinction $A_K > 1.0$ mag. Adapted from Clarke *et al.* (2019).

Including the new PM data into these made-to-measure models is expected to lead to much tighter constraints on the dynamics of the Galactic bulge.

References

- Benjamin, R. A., Churchwell, E., Babler, B. L., *et al.* 2005, *ApJL*, 630, L149
 Clarke, J. P., Wegg, C., Gerhard, O., Smith, L. C., & Lucas, P. W., 2019, *MNRAS* 489, 3519
 Gerhard, O. 2018, *IAUS* 334, 73
 Hammersley, P. L., Garzón, F., Mahoney, T. J., *et al.* 2000, *MNRAS*, 317, L45
 Kozłowski, S., Woźniak, P. R., Mao, S., *et al.* 2006, *MNRAS*, 370, 435
 Kunder, A., Koch, A., & Rich, R. M., *et al.* 2012, *AJ*, 143, 57
 McWilliam, A. & Zoccali, M. 2010, *ApJ*, 724, 1491
 Molaeinezhad, A., Falcón-Barroso, J., & Martínez-Valpuesta, I., *et al.* 2016, *MNRAS*, 456, 692
 Nataf, D. M., Udalski, A., Gould, A., Fouqué, P., & Stanek, K. 2010, *ApJ*, 721, L28
 Ness, M., Freeman, K., Athanassoula, E., *et al.* 2013, *MNRAS*, 432, 2092
 Ness, M., Zasowski, G., Johnson, J. A., *et al.* 2016, *ApJ* 819, 2
 Portail, M., Wegg, C., Gerhard, O., & Martinez-Valpuesta, I. 2015, *MNRAS*, 448, 713
 Portail, M., Gerhard, O., Wegg, C., & Ness, M. 2017a, *MNRAS*, 465, 1621 (P17a)
 Portail, M., Wegg, C., Gerhard, O., & Ness, M. 2017b, *MNRAS*, 470, 1233 (P17b)
 Rattenbury, N. J., Mao, S., Debattista, V. P., *et al.* 2007, *MNRAS*, 378, 1165
 Sanders, J. L., Smith, L., Evans, N. W., & Lucas, P. W., 2019, *MNRAS*, 487, 5188
 Shen, J., Rich, R. M., Kormendy, J., *et al.* 2010, *ApJ*, 720, L72
 Smith, L. C., Lucas, P. W., Kurtev, R., *et al.* 2018, *MNRAS*, 474, 1826
 Sormani, M. C., Binney, J., & Magorrian, J. 2015, *MNRAS*, 454, 1818
 Stanek, K. Z., Mateo, M., Udalski, A., *et al.* 1994, *ApJL*, 429, L73
 Wegg, C. & Gerhard, O. 2013, *MNRAS* 435, 1874
 Wegg, C., Gerhard, O., & Portail, M. 2015, *MNRAS* 450, 4050
 Zoccali, M., Vasquez, S., Gonzalez, O. A., *et al.* 2017, *A&A*, 599, 12